Nitrososynthase triggered oxidative carbon-carbon bond cleavage in baumycin biosynthesis

Ahmad Al-Mestarihi,[1] Anthony Romo,[2] Hung-wen Liu,[2] and Brian O. Bachmann[1,*]

[1]*Vanderbilt University Department of Chemistry, Nashville TN 37235*

[2]*Division of Medicinal Chemistry, College of Pharmacy and Department of Chemistry and Biochemistry, University of Texas at Austin, Austin, TX 78712*

Supplementary Data Table of Contents

Bacterial strains, Plasmids and Materials. All reagents were obtained from Sigma-Aldrich Corporation and used without further purification unless otherwise noted. *E. coli* TOP10 and BL21 (DE3) competent cells were obtained from Invitrogen Inc. (Carlsbad, CA) and Novagen (Madison, WI), respectively. Restriction endonucleases and T4 DNA ligase were obtained from New England Biolabs (Ipswich, MA). The pET28a expression vector was purchased from Novagen Inc. *Taqplus* DNA polymerase was purchased from Stratagene Inc. (La Jolla, CA).

Cloning and overexpression of DnmZ. The gene encoding DnmZ enzyme (Gene Bank Accession AAB63045.1) was amplified from the genomic DNA of *Streptomyces peucetius* (ATCC 29050) using the following primers 5'- CATATGACAAAGCCATCTGTGCACG-3' and 5'- AAGCTTTCATCGGCCCAACGCCACTT-3' (*Nde*I and *Hind*III restriction enzyme sites underlined). Polymerase chain reaction (PCR) was carried out using *Taqplus* DNA polymerase according to the manufacture's protocol. Subcloning of *dnmZ* into the *Nde*I/*Hind*III sites of pET28a yielded recombinant plasmid pET28-ZN for expression as an *N*-terminal hexahistidine fusion protein. Plasmid pET28-ZN was transformed by electroporation into *E. coli* BL21(DE3) for heterologous expression of DnmZ. Cultures of *E. coli* BL21(DE3)/pET28-ZN (1 L) were grown at 37 °C to an OD_{600} of 0.6, at which point the culture was induced with 0.1 mM isopropyl-beta-D-thiogalactopyranoside (IPTG) and grown for additional 6 hours at 28 °C. Cells were harvested by centrifugation and stored at -80 °C until needed. IPTG induced *E. coli* BL21(DE3)/pET28-ZN cells were resuspended in buffer A (20 mM imidazole, 0.5 M NaCl, 20 mM Tris-Cl, pH 7.5) and lysed via passage through a French pressure cell at 20,000 psi. The lysate was loaded onto a charged 5-mL Histrap (Ni^{+2}-affinity) crude column (Amersham Biosciences) and purified by fast protein liquid chromatography (FPLC) at a flow rate of 5 mL/min. The column was washed with buffer A (20 mM imidazole, 0.5 M NaCl, 20 mM Tris-Cl, pH 7.5) and buffer B (500 mM Imidazole, 0.5 M NaCl, 20 mM Tris-Cl, pH 7.5) using a step gradient. Fractions containing DnmZ purified to homogeneity as analyzed by SDS-PAGE (Figure S1) were pooled and buffer was exchanged via a desalting column (Highprep, from Amersham Biosciences) using buffer C (20 mM Tris-Cl, 1 mM dithiothreitol (DTT) and 5% glycerol, pH 7.5) and stored at -80 °C until assayed.

Cloning and overexpression of DnrH. The gene encoding DnrH enzyme (Gene Bank Accession AAD04714.1) was amplified from the genomic DNA of S*treptomyces peucetius* (ATCC 29050) using the following primers 5'-CATATGCGCGTCCTGTTCGCCA-3' and 5'-AAGCTTCTAGGCACCGCCGG-3' (*Nde*I and *Hind*III restriction enzyme sites underlined). Subcloning of *dnrH* into pET28a expression vector was performed as described for *dnmZ* above. One liter cultures of *E. coli* BL21(DE3) harboring the expression vector were incubated at 37 °C to an OD_{600} of 0.6, at which point the temperature was lowered to 30 °C and the cultures were allowed to incubate overnight for 12 h. Protein purification was performed as described above for DnmZ. SDS-PAGE analysis of the fractions containing the desalted DnrH protein displayed multiple proteins with the most abundant band corresponded to the molecular weight of DnrH enzyme.

Cloning and overexpression of RubN7. The gene encoding the C4-*O*-methyltransferase RubN7 (Gene Bank Accession CAI94729.1) was amplified from the genomic DNA of *Streptomyces achromogenese var. rubradiris* (NRRL3061) using the following primers 5'-TCCATATGACCGGTCAGGTGCACCGGC-3' and 5'-TCAAGCTTTCACCGCGGCACCGCCC-3' (*Nde*I and *Hind*III restriction enzyme sites underlined). Subcloning of *rubN7* into pET28a expression vector was performed in the same way described for *dnmZ* above. One liter cultures of *E. coli* BL21(DE3) harboring the expression vector were grown at 37 °C to an OD_{600} of 0.6, at which point the temperature was lowered to 30° C and the cultures were allowed to grow for additional 8 h. The protein was purified to homogeneity via FPLC using Ni^{2+}-affinity column as described above for DnmZ.

LC-ESI-MS Method for structure identification and enzymatic assays. DnmZ assays were analyzed using Thermo Finnigan (San Jose, CA) TSQ® Quantum triple quadrupole mass spectrometer equipped with a standard electrospray ionization source outfitted with a 50 μm inside diameter deactivated fused silica capillary. Injections of 10 μL were separated using a Hypercarb column (3 mm ×the 50 mm, Thermo Inc.). Mobile phases were (A) H_2O with 50 mM ammonium formate and 0.1% (v/v) diethylamine and (B) a H_2O/acetonitrile mixture (5:95) with 50 mM ammonium formate and 0.1% (v/v) diethylamine. Gradient conditions were as follows: linear gradient from 0 to 100% B for 30 min, washing with 100% B from 30 to

40 min and, equilibrating with 100% A from 40 to 50 min. The flow rate was maintained at 0.2 mL/min. The mass spectrometer was operated in both the negative and positive ion full scan profile modes, and the electrospray needle was maintained at 3100 V. The ion transfer tube was operated at -47.50 V and 275 °C. The tube lens voltage was set to -46 V. The collision energy for all product ion scans was set at 25%.

Preparation of TDP-L-*epi*-vancosamine. TDP-L-epivancosamine was biochemically synthesized from thymidine-5'-diphospho-α-D-glucose using procedures adapted from Chen *et al*. The following enzymes were used to transform thymidine-5'-diphospho-α-D-glucose to TDP-L-epivancosamine: RfbB from the rhamnose biosynthetic pathway, Eva A-E from the chloroeremomycin biosynthetic pathway. The last step of this biosynthesis was modified as follows: TDP-L-epivancosamine was generated from its TDP-4-keto-3-amino sugar precursor (1 mM) in a 1-mL reaction containing 100 mM Tris-HCl (pH 7.5), 5 mM NADPH, 20 µM EvaD and 50 µL of the resuspended EvaE pellet. The reaction was incubated at 24 °C for 2 h, proteins and cell debris were removed using a 10K centrifugal filter (Centricon), and the product was purified by SAX-HPLC (described below) followed by lyophilization which resulted in ~300 µg of semi-pure TDP-L-*epi*-vancosamine. ESI-LC MS analysis (Figure S2) confirmed the mass of TDP-L-epivancosamine (*m*/*z* found 544.27). Further confirmation of the structure was performed via tandem MS analysis which showed fragment ions corresponding to TDP at *m*/*z* 401 and *m*/*z* 383.

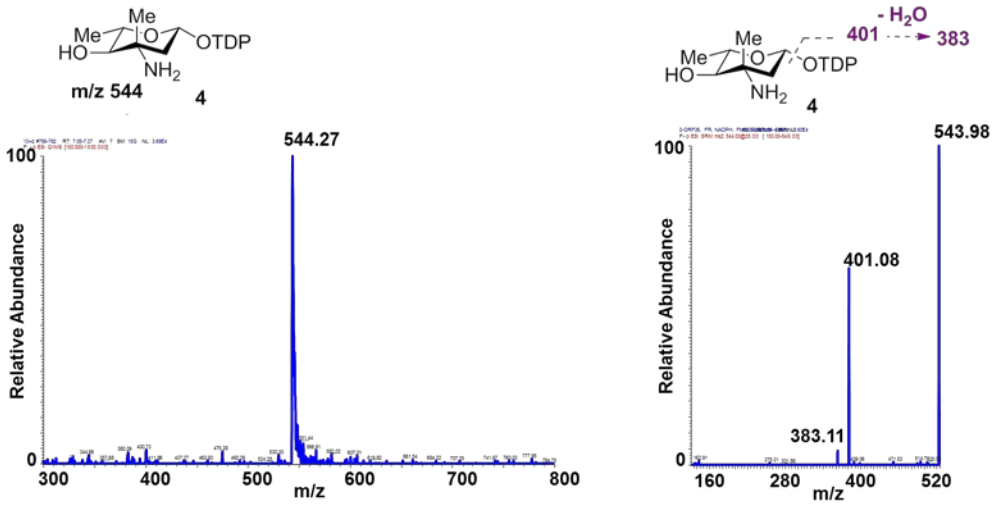

Figure S1. MS and tandem MS of TDP-L-vancosamine (4). Shown spectra are MS (left) and MS/MS (right). Suggested fragment ions are shown above the MS/MS spectra.

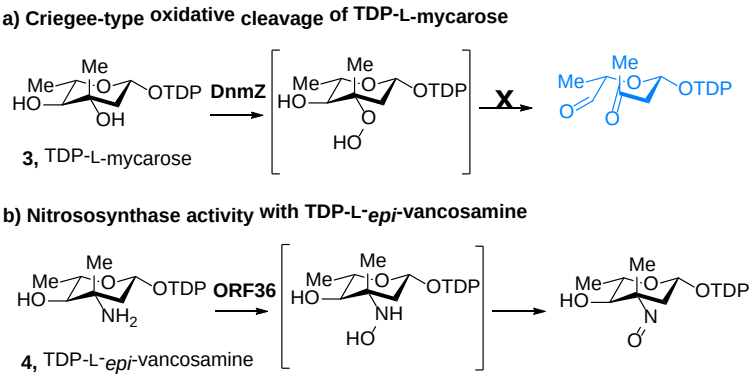

Figure S2. Proposed DnmZ oxidation of TDP-L-mycarose.

Purification of TDP-L-*epi*-vancosamine. Preparative enzymatic reaction progress was followed via HPLC using a series 600 Wat-L-ers HPLC system with a Waters 2996 diode array detector. Analytical separations were performed on an Adsorbosphere strong anion exchange (SAX) column (5 µm, 4.6 mm × 20 mm, Alltech Associates) and a linear gradient from 50 to 500 mM ammonium formate (pH 3.5) at 1 mL/min for 45 min. Preparative HPLC separations were performed using a semipreparative Adsorbosphere SAX column (5 µm, 22 mm 250 mm) using a similar protocol, but at 10 mL/min. The pH values of the fractions containing TDP chromophores (267 nm) were immediately adjusted to ~7 with 1 M NH_4OH, and fractions containing reaction product were pooled, lyophilized, and stored at -80 °C until assayed. Resuspended compound concentrations were determined by measurement of the absorbance at 267 nm using a Nanodrop spectrophotometer (Thermo, Inc.) and comparison to a standard curve of TDP.

Preparation of TDP-L-evernosamine. TDP-L-evernosamine was enzymatically generated from TDP-L-*epi*-vancosamine as follows: in a 100 µL reaction of pH 7.5 containing TDP-L-*epi*-vancosamine (100 µM), 100 mM Tris-HCl, 10 mM S-adenosylmethionine (SAM), and 50 µM RubN7. The reaction was incubated at 24 °C for 2 h. Protein and cell debris were removed using a 10K centrifugal filter (Centricon). ESI-LC MS (Figure S4) confirmed the mass of TDP-L-evernosamine ($[M-H]^-$ LRMS calculated for $C_{18}H_3N_3O_{13}P_2^-$ is 558.13, found 558.07. The MS/MS of the product showed typical TDP fragment ion at *m*/*z* 401, 383 ($-H_2O$). The reaction mixture was used without further purification for DnmZ and ORF36 assays with TDP-L-evernosamine.

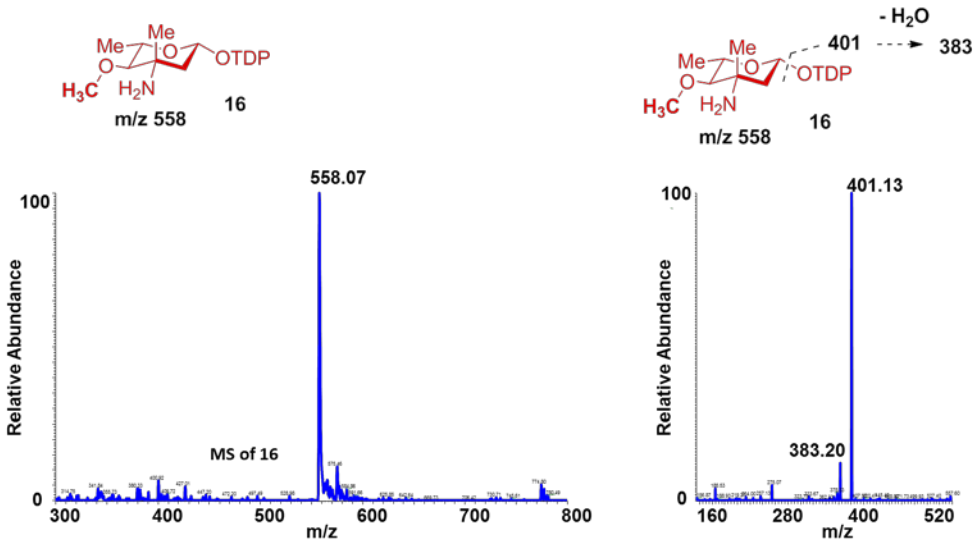

Figure S3. MS and tandem MS of TDP-L-evernosamine (16). Shown spectra are MS (left) and MS/MS (right). Suggested fragment ions are shown above the MS/MS spectra (selected ion = 558).

Preparation and purification of TDP-L-mycarose. The enzymes involved in the TDP-L-mycarose biosynthetic pathway (Figure S4) were purified as reported [1,2], and *in vitro* biosynthesis was carried out essentially as published [1].

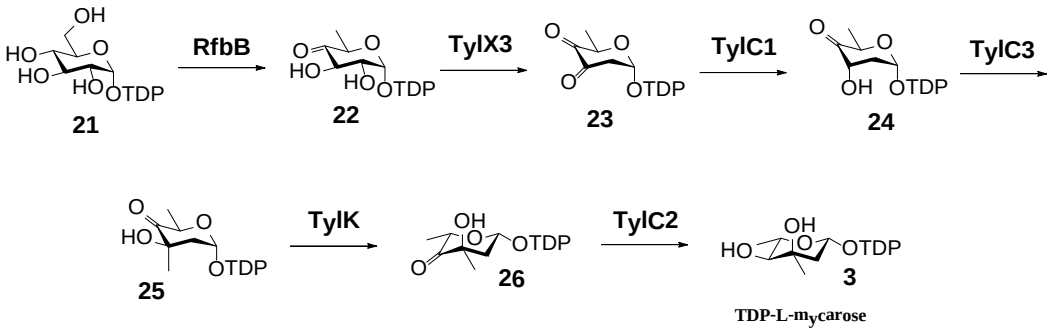

Figure S4. The biosynthetic pathway utilized to prepare TDP-L-mycarose.

Specifically, TDP-4-keto-6-deoxyglucose was generated using 5 mM TDP-glucose, 30 μM RfbB [3], and 100 μM NAD^+ in 50 mM TRIS base, pH 7.0, at 37 °C for 45 min. Then TylC1, TylC3, TylC2, and TylK were added each to a final concentration of 30 μM, whereas TylX3 was added to a concentration of 20 μM; NADPH and SAM were added to a final concentration of 10 mM. This reaction was incubated at 30 °C for 1 h. Reaction progress was monitored by HPLC (Dionex Carbopac analytical column; 267 nm; A: water,

B: 500 mM ammonium acetate in water; 5%-20% B over 15 min, 20%-60% B over 20 min, 60%-100% B over 2 min, hold 3 min, 100%-5% B over 5 min) (Figure S6), and the identity of TDP-mycarose was confirmed by HRESI(-) mass spectrometry. For DnrH assays, TDP-mycarose was purified on a larger scale using semi-preparatory HPLC (Dionex Carbopac Semi-Prep column) and once again confirmed through ESI(-) mass spectrometry (Figure S7).

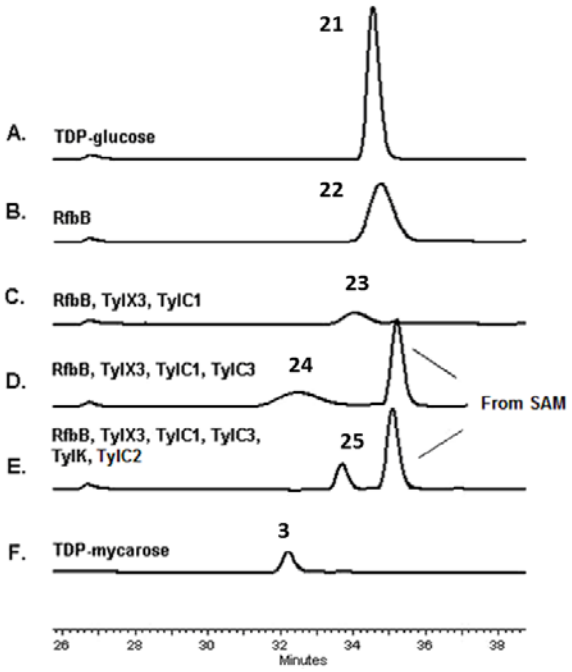

Figure S5. HPLC analysis of the enzymatic synthesis of TDP-L-mycarose.

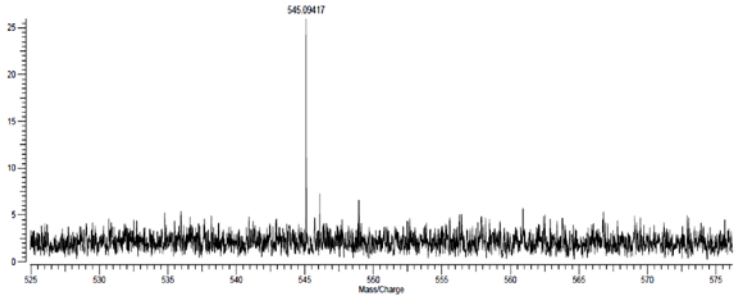

Figure S6. High resolution ESI(-) MS of TDP-L-mycarose.

DnmZ/ORF36 assay with TDP-L-*epi*-vancosamine. Reactions of DnmZ with TDP-L-epivancosamine were performed in a total volume of 50 μL containing 30 μM TDP-L-epivancosamine, 30 μM FAD, 1 U/mL catalase from bovine liver, 1 U/mL Horseradish superoxide dismutase , 0.4 U/mL flavin reductase from *V.*

fischeri, and 2.0 mM NADPH. All reactions were initiated by addition of 15 μM DnmZ or ORF36 and reactions were quenched with equal volume of acetone, and mixtures stored at -80 °C until analyzed by LC-ESI-MS. Control assays, performed in the absence of either DnmZ, ORF36, FAD, or NADPH, showed no product formation. Figure S8 shows the MS and MS/MS of the DnmZ reaction products and suggested structures of the tandem MS fragment ions.

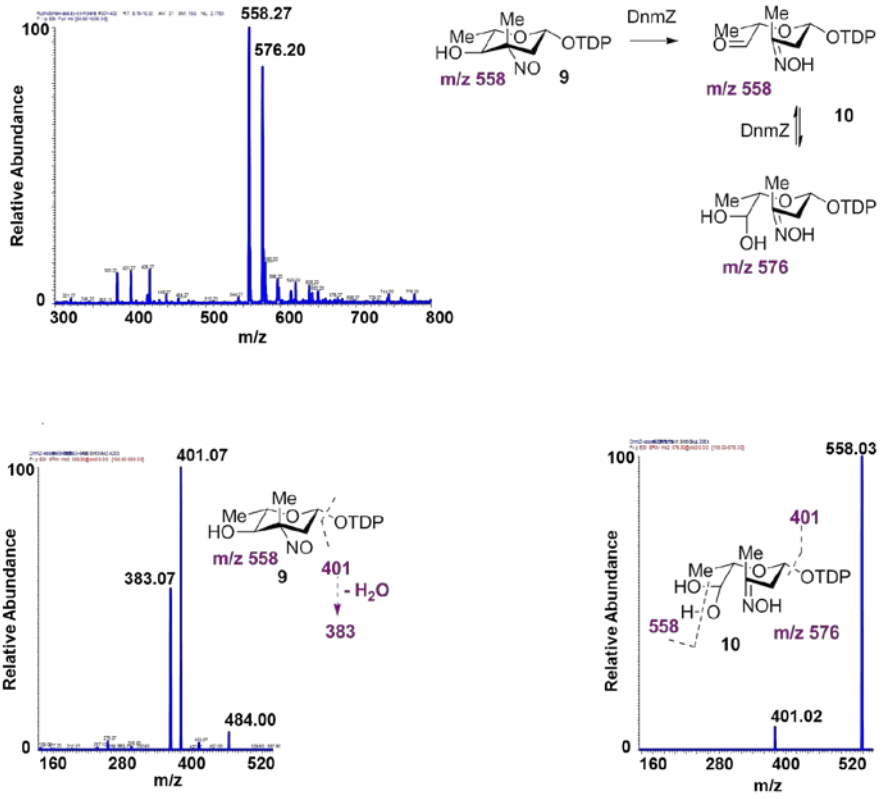

Figure S7. MS and tandem MS of DnmZ reaction products. Shown spectra are MS (above) and MS/MS (below) of reaction products 9 and 10. Suggested fragment ions are shown in the MS/MS spectra.

DnmZ and ORF36 assays with TDP-L-evernosamine. Reactions of DnmZ and ORF36 with TDP-L-evernosamine were performed in a total volume of 50 μL containing 30 μM TDP-L-evernosamine, 30 μM FAD, 1 unit/mL catalase from bovine liver, 1 U/mL Horseradish superoxide dismutase, 0.4 U/mL flavin reductase from *V. fischeri*, and 2.0 mM NADPH. All reactions were initiated by addition of 15 μM DnmZ or ORF36. Reactions were quenched with equal volume of acetone, and mixtures stored at -80 °C until

analyzed by LC-ESI-MS (Figures S9, S10). Control assays, performed without DnmZ, ORF36, FAD, or NADPH showed no reaction products.

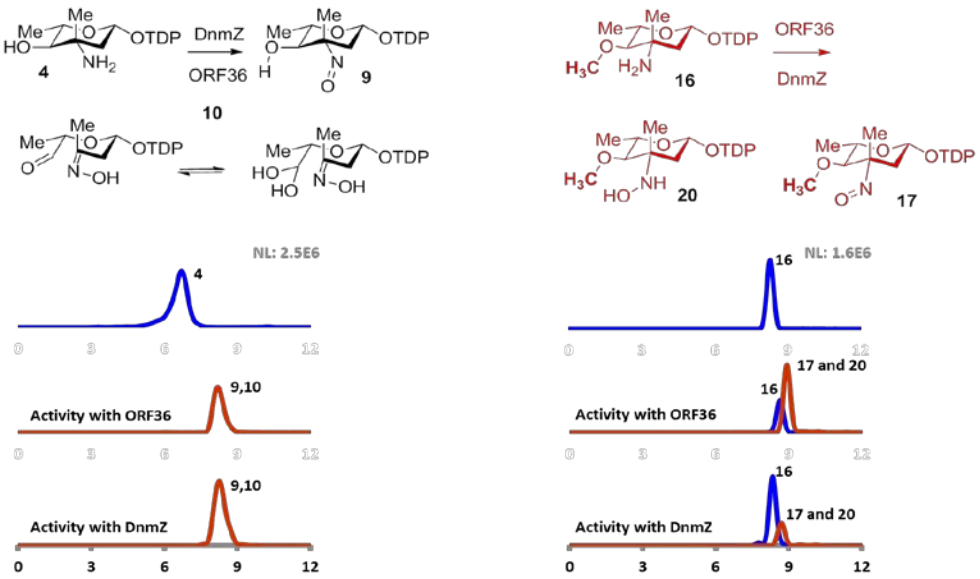

Figure S8. HPLC-MS chromatograms of ORF36 and DnmZ activities with TDP-L-epi-vancosamine (left) and TDP-L-evernosamine (right). Under identical reaction conditions, ORF36 reacts more completely with TDP-L-evernosamine than DnmZ

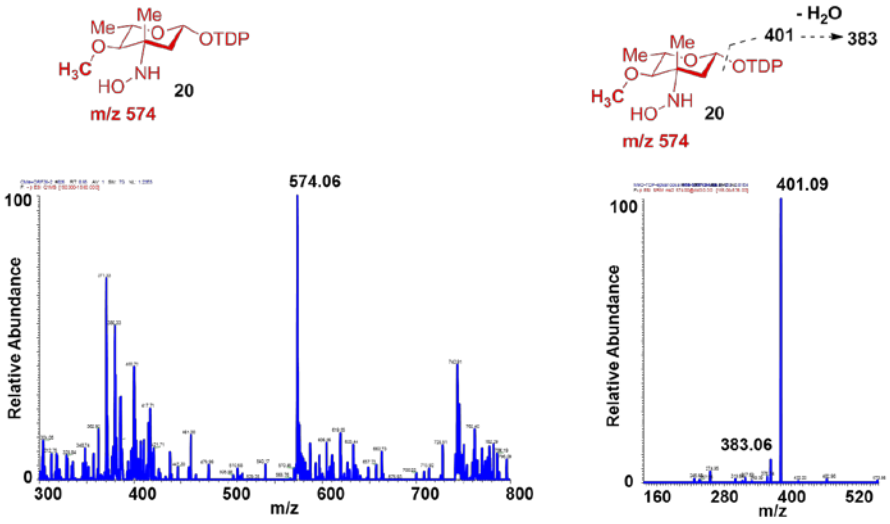

Figure S9. MS and tandem MS analysis of Dnmz reaction with TDP-L-evernosamine. Spectra shown are MS (left) and MS/MS (right) of the hydroxylamine product 20. Suggested fragment ions are shown above the MS/MS spectra.

DnrH assays. The glycosyltransfer DnrH reactions were performed at pH 7.0 in a mixture containing 10% glycerol in 50 mM Tris-base, 100 μM TDP-mycarose, 1 mM $MgSO_4$, 66 μM daunorubicin HCl, and 10 μM DnrH at room temperature, 30 °C, and 37 °C. None of these conditions showed new products.

Derivatization of DnmZ products with hydrazines. Upon completion of the DnmZ reaction with TDP-L-*epi*-vancosamine, the reaction mixture (50 uL) was incubated with the corresponding hydrazine (1 mM) for 2 h at room temperature. The mixture was kept at - 80 °C until analyzed by HPLC-MS. The following hydrazines were used for the derivatization experiments: phenylhydrazine, 2-bromophenylhydrazine, and Girard's reagent (carboxymethyl)trimethylammonium chloride hydrazide; 2-hydrazino-*N*,*N*,*N*-trimethyl-2-oxo-ethanaminium chloride). As expected, all hydrazines reacted with the oxime-aldehyde compound **10** to form the corresponding hydrazone adduct. Figures S11 and S12 show the MS and tandem MS analysis of these adducts.

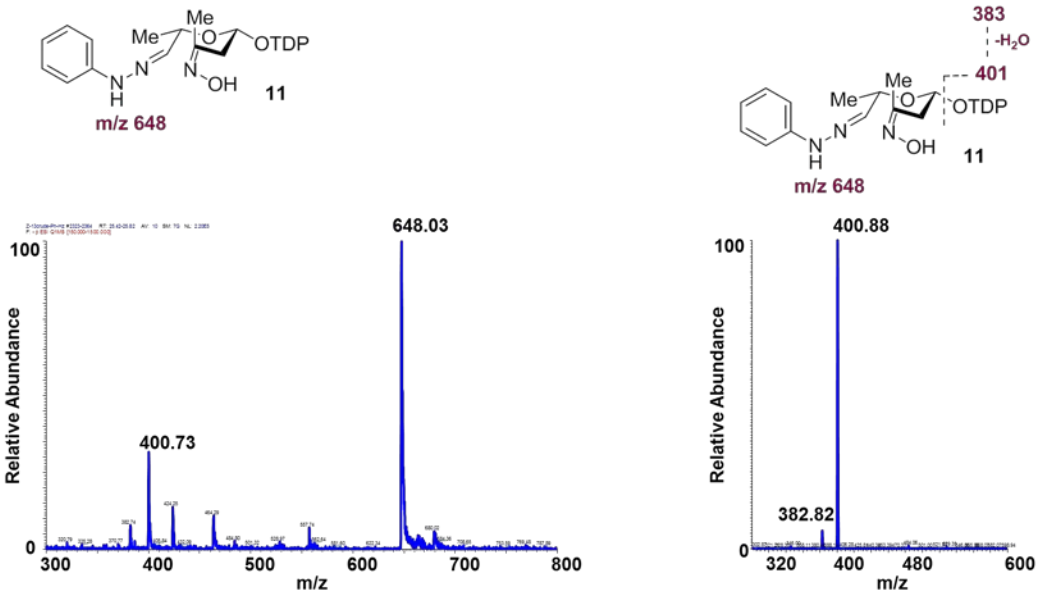

Figure S10. MS and tandem MS of the phenyl hydrazone adduct 11. Shown spectra are MS (left) and MS/MS (right) for the species of *m*/*z* 648 corresponding to the shown structure. Suggested ions are shown above the MS/MS spectra.

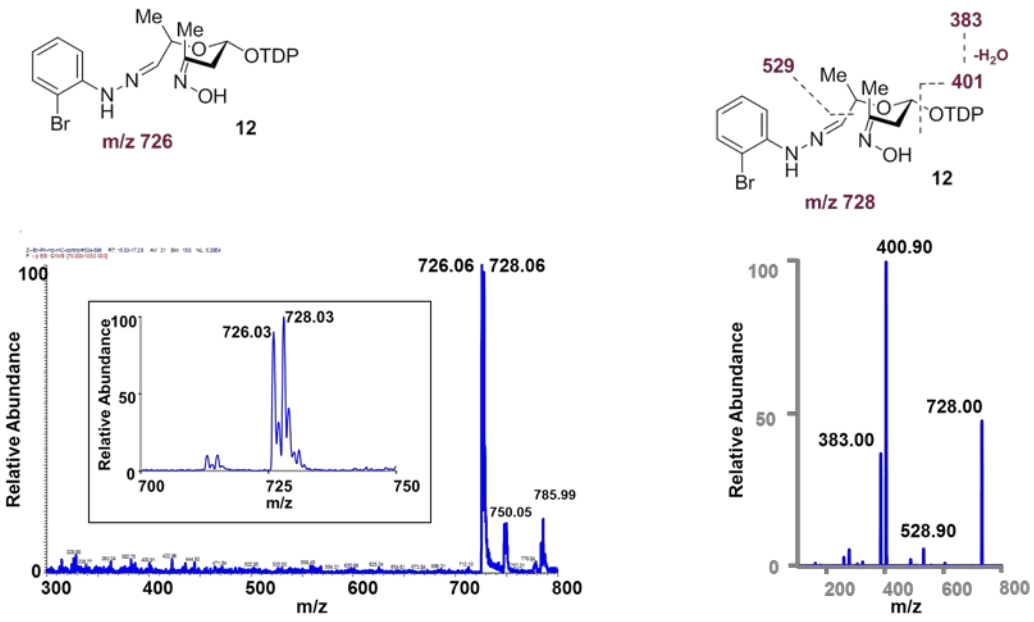

Figure S11. MS and tandem MS of the 2-bromophenyl hydrazone adduct 12**.** Shown spectra are MS (left) and MS/MS (right) of the shown structure (*m/z* 726). The insert in the left spectra is MS obtained from single ion monitoring of the species of *m/z* 726 and 728 corresponding to the isotopic distribution of 2-bromophenyl hydrazone adduct. Suggested fragment ions are shown above the MS/MS spectra.

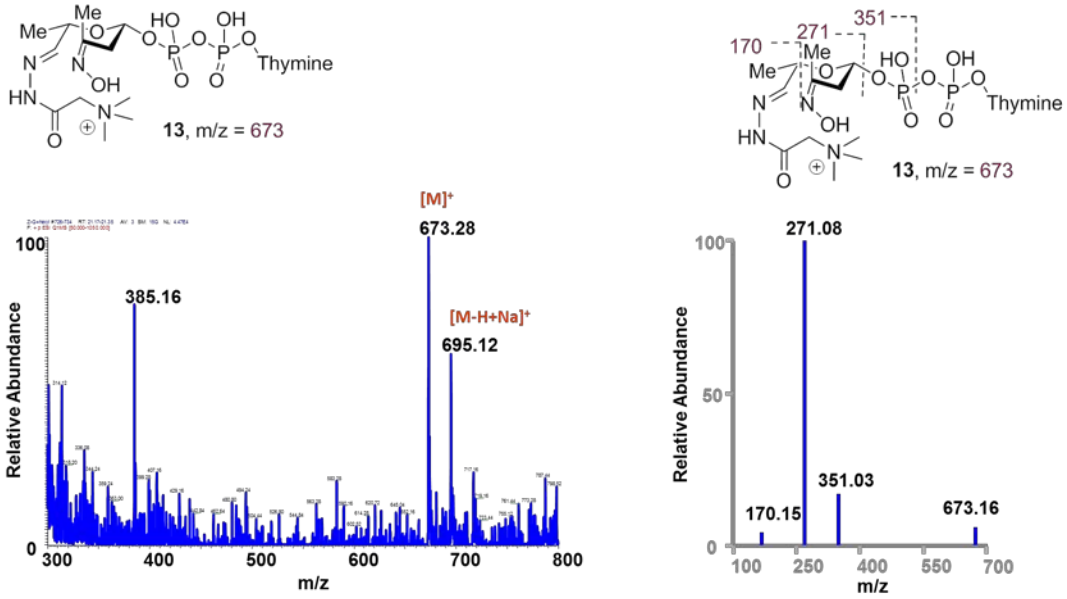

Figure S12. MS and tandem MS of the GirT hydrazide adduct 13. Shown spectra are MS (left) and MS/MS (right). Analysis was performed in the positive ion mode. Suggested fragment ions are shown above the MS/MS spectra.

Acid hydrolysis of the GirT hydrazide. Acid hydrolysis of the GirT hydrazide adduct **13** was performed as follows: 10 µL of 5M HCl was added to 40 µL of the crude mixture containing the GirT hydrazide **13**

and the hydrolysis reaction was allowed to proceed for 2 h at room temperature. The mixture was kept at -80 °C until analyzed by HPLC-MS. Figure S14 shows the MS and tandem MS of the resulting acid hydrolysis products.

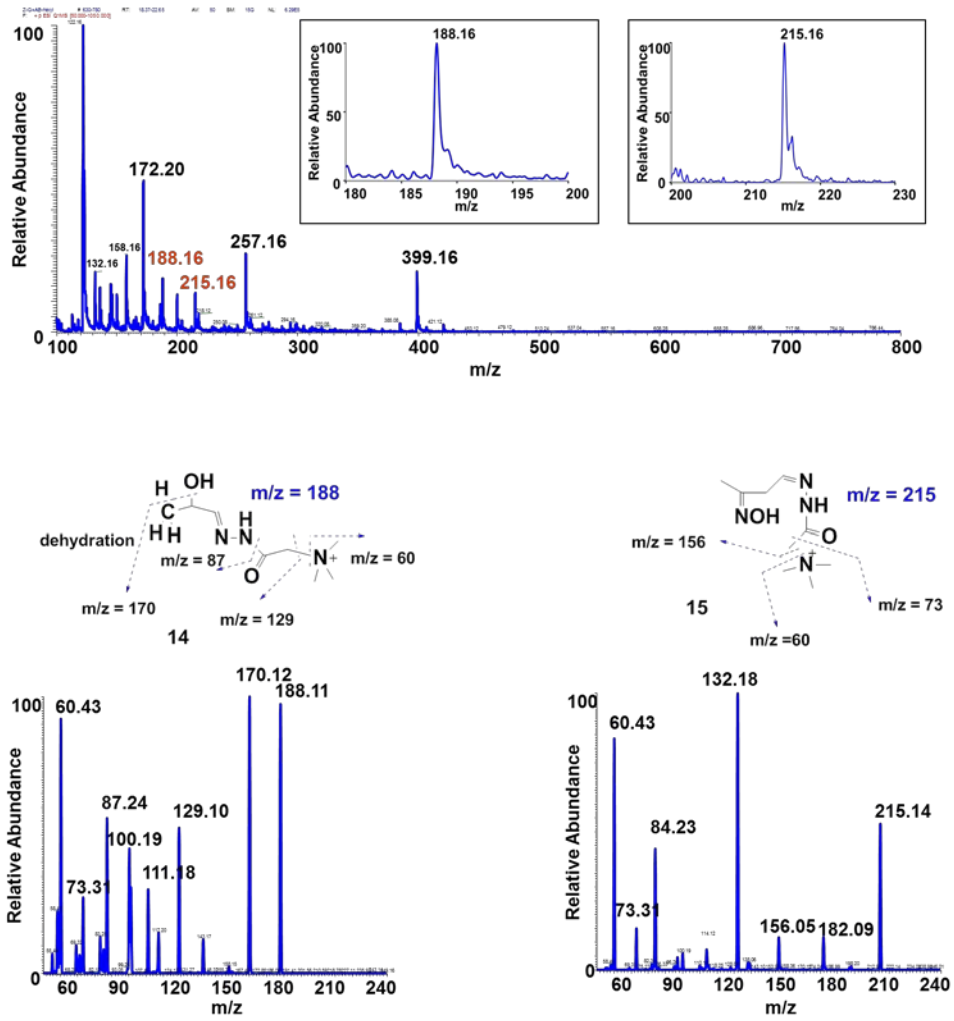

Figure S13. MS (above) and tandem MS (below) of the acid hydrolysis products 14 and 15 from the acid treated GirT hydrazide adduct**.** Suggested fragment ions are shown above each MS/MS spectra. Inserts in the above spectra are MS obtained from single ion monitoring for the species of *m/z* 188 and 215 corresponding to compounds 14 and 15.

High resolution mass measurements and structure eluicidation. High resolution LC-MS analyses of the hydrazone adducts were carried out using a Synapt hybrid quadrupole/oa-TOF Mass Spetrometer (Waters Corp., Milford, MA) equipped with a dual chemical ionization/electrospray (ESCI) source and interfaced with a Waters Acquity UPLC system (Waters, Milford, MA). The TOF analyzer was calibrated in both

positive and negative V modes over a mass range of 50-1000 m/z using a solution of sodium formate following the manufacturer's recommended procedure. A gain correction was applied during data acquisition using a solution of CHAPS buffer ([M+K+]+ (exact mass 653.3596) in the lock channel. An Atlantis C18 column (2.1 mm × 100 mm, 3 mm) (Waters, Milford MA) was used for all chromatographic separations. Mobile phases were (A) H_2O with 50 mM ammonium formate and 0.1% (v/v) diethylamine and (B) a H_2O/acetonitrile mixture (5:95) with 50 mM ammonium formate and 0.1% (v/v) diethylamine. Gradient conditions were as follows: linear gradient from 0 to 100% B from for 30 min, 100% B from 30 to 40 min, 100% A from 40 to 50 min. The flow rate was maintained at 0.2 mL/min. The autosampler injection valve and the sample injection needle were flushed and washed sequentially with mobile phase B (0.5 mL) and mobile phase A (1 mL) between each injection. The autosampler tray temperature was set to 25 °C. As shown in Figure S15, mass accuracies of less than 3.00 ppm were confirmed for all of the hydrazone conjugates and their intermediate precursors measured. Taken together, these high resolution mass measurements are consistent with the assigned structures of the TDPlinked hydrazones and their sugar nucleotide precursors and are in support of the proposed oxime-aldehyde product **10** resulting from deoxysugar C-C bond cleavage triggered by DnmZ activity.

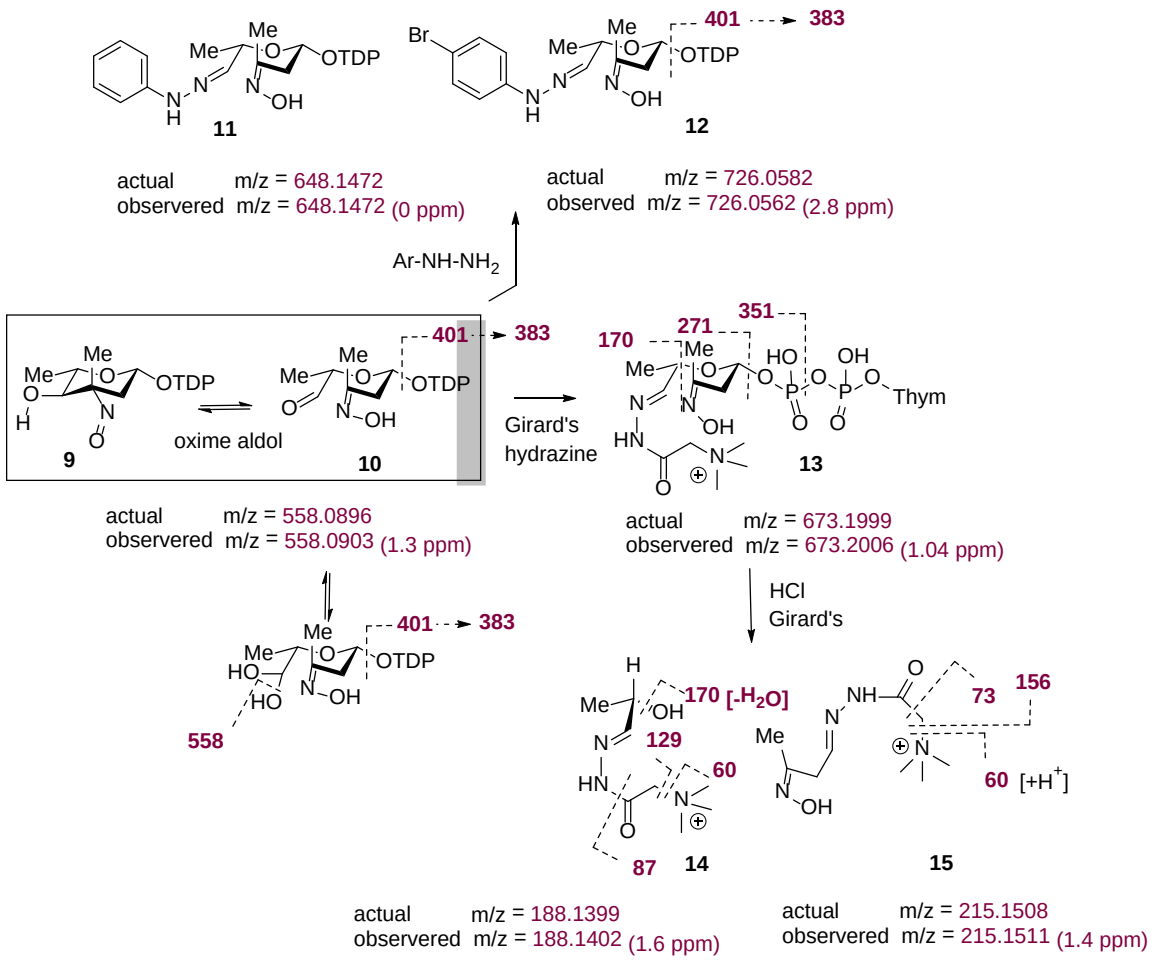

Figure S14. Summary of structural analysis of oxime aldol product 9/10 and high resolution mass measurements of the hydrazone adducts.

References:

[1] H. Takahashi, Y.-n. Liu, H.-w. Liu. A two-stage one-pot enzymatic synthesis of TDP-L-mycarose from thymidine and glucose-1-phosphate. *J. Am. Chem. Soc.* 128 (**2006**) 1432-1433.

[2] H. Takahashi, Y.-n. Liu, H. Chen, H.-w. Liu. Biosynthesis of TDP-L-mycarose: the specificity of a single enzyme governs the outcome of the pathway. *J. Am. Chem. Soc.* 127 (**2005**) 9340-9341.

[3] J. White-Phillip, C.J. Thibodeaux, H.-w. Liu. Enzymatic synthesis of TDP-sugars. Methods *Enzymol.* 459 (**2009**) 521-544.